



2 Application of TopoFlow, a spatially distributed hydrological model, to 3 the Innavaik Creek watershed, Alaska

4 Imke Schramm,¹ Julia Boike,¹ W. Robert Bolton,² and Larry D. Hinzman³

5 Received 26 September 2006; revised 11 January 2007; accepted 6 April 2007; published XX Month 2007.

6 [1] This study presents the application of the hydrological model TopoFlow to the
7 Innavaik Creek watershed, Alaska, United States. It summarizes the hydrologically
8 important processes in this arctic basin, and focuses on the modeling of the hydrological
9 processes in 2001. The model is evaluated for its capability to reproduce the different
10 components of the hydrological cycle. Model simulations are done for different climate
11 change scenarios to evaluate the impacts on the hydrology. Innavaik Creek ($\sim 2 \text{ km}^2$) is
12 underlain by continuous permafrost, and two features characterize the channel network:
13 The stream is beaded, and numerous water tracks are distributed along the hillslopes.
14 These facts, together with the constraint of the subsurface system to the shallow active
15 layer, strongly influence the runoff response to rain or snowmelt. Climatic conditions vary
16 greatly during the course of the year, providing a good testing of model capabilities.
17 Simulation results indicate that the model performs quantitatively well. The different
18 components of the water cycle are represented in the model, with refinements possible in
19 the small-scale, short-term reproduction of storage-related processes, such as the beaded
20 stream system, the spatial variability of the active layer depth, and the complex soil
21 moisture distribution. The simulation of snow melt discharge could be improved by
22 incorporating an algorithm for the snow-damming process.

23 **Citation:** Schramm, I., J. Boike, W. R. Bolton, and L. D. Hinzman (2007), Application of TopoFlow, a spatially distributed
24 hydrological model, to the Innavaik Creek watershed, Alaska, *J. Geophys. Res.*, *112*, XXXXXX, doi:10.1029/2006JG000326.

26 1. Introduction

27 1.1. Hydrology of the Arctic

28 [2] The presence of permafrost is the primary factor
29 distinguishing arctic from temperate watersheds. Permafrost
30 underlies approximately 24% of the exposed land area in the
31 Northern Hemisphere, making it a significant proportion of
32 the land mass [Romanovsky *et al.*, 2002]. The permafrost
33 condition is a crucial component in its influence on many of
34 the hydrologic processes in the arctic and subarctic environ-
35 ments. The presence of permafrost significantly alters
36 surface and subsurface water fluxes, as well as vegetative
37 functions [Walsh *et al.*, 2005]. Permafrost dominates micro-
38 climatology and the thermal regime, including evapotrans-
39 piration [Hinzman *et al.*, 1996, 2006]. Permafrost controls
40 water storage processes and the energy and water balances
41 [Boike *et al.*, 1998; Bowling *et al.*, 2003].

42 [3] Hinzman *et al.* [2005] point out that the primary
43 control on hydrological processes is dictated by the pres-
44 ence or absence of permafrost, but is also influenced by the
45 thickness of the active layer, the thin layer of soil overlying

permafrost that thaws in the summer. The active layer in the 46
arctic varies from several tens of centimeters to 1 or 2 m in 47
depth. It is of pivotal importance, as most hydrological and 48
biogeochemical processes occur in this zone [Kane *et al.*, 49
1991a; Walsh *et al.*, 2005]. The conditions for plant growth, 50
gas fluxes, groundwater flow regimes, and soil formation 51
are all limited and to some extent determined by the active 52
layer [Boike *et al.*, 1998]. The permafrost beneath the active 53
layer limits the amount of soil water percolation and 54
subsurface storage of water [Vörösmarty *et al.*, 2001]. 55
Whereas nonpermafrost soils allow a deep groundwater 56
system, the subsurface movement of water in permafrost- 57
affected soils is largely confined to the shallow active layer. 58
Therefore lateral flow is more important than in nonperma- 59
frost soils [Slaughter and Kane, 1979]. These characteristics 60
have a large impact on the runoff response. Permafrost 61
generally accelerates the initiation of runoff [McNamara *et* 62
al., 1998]. As the water movement through the near-surface 63
soils is relatively fast, the runoff response to precipitation is 64
characterized by a rapid rise to peak flow and a rapid 65
decline following peak flow [Dingman, 1973]. In addition, 66
response times are shortened because vegetation in these 67
areas tends to be sparse [Church, 1974]. While permafrost- 68
dominated watersheds generally have a larger contributing 69
area and a higher specific discharge, the specific base flow 70
is lower compared to nonpermafrost regions [McNamara *et* 71
al., 1998]. 72

[4] The annual thawing and freezing of the active layer 73
are the driving forces for many surficial processes, such as 74

¹Alfred Wegener Institute for Marine and Polar Research, Potsdam, Germany.

²Water and Environmental Research Center, University of Alaska, Fairbanks, Fairbanks, Alaska, USA.

³International Arctic Research Center, University of Alaska, Fairbanks, USA.

75 cryoturbation. These perennial processes also have a control
 76 on the hydraulic properties of the soil, specifically the
 77 storage capacity and hydraulic conductivity [Hinzman *et*
 78 *al.*, 1991]. The variation of hydraulic properties results in
 79 runoff patterns which change throughout the thaw season.
 80 To understand hydrologic dynamics of the arctic, it is
 81 conducive to study the seasonal change in soil moisture in
 82 the active layer. An overview over the seasonal active layer
 83 characteristics is given in section 2.

84 1.2. Arctic Hydrology in a Changing Climate

85 [5] Air temperature, snow cover, and vegetation, all of
 86 which are affected by climate change, affect the temperature
 87 of the frozen ground and the depth of seasonal thawing. In
 88 interior Alaska, United States, the warmer climate has led to
 89 shrinking permafrost coverage and an increased active layer
 90 depth [Osterkamp and Romanovsky, 1999].

91 [6] General circulation models predict that the effects of
 92 anthropogenic greenhouse warming will be amplified in the
 93 northern high latitudes due to feedbacks in which variations
 94 in snow and sea ice extent, the stability of the lower
 95 troposphere, and thawing of permafrost play key roles
 96 [Serreze *et al.*, 2000]. Over the next 100 a the observed
 97 changes are projected to continue and their rate to increase,
 98 with permafrost degradation estimated to occur over 10–
 99 20% of the present permafrost area, and the southern limit
 100 of permafrost expected to shift northward by several hun-
 101 dred kilometers [ACIA, 2004].

102 [7] A progressive increase in the depth of seasonal
 103 thawing could be a relatively short-term reaction to climate
 104 change in permafrost regions, since it does not involve any
 105 lags associated with the thermal inertia of the climate/
 106 permafrost system [Walsh *et al.*, 2005]. There is a general
 107 consensus among models that seasonal thaw depths are
 108 likely to increase by more than 50% in the northernmost
 109 permafrost locations [Walsh *et al.*, 2005]. It appears that
 110 first-order impacts to the arctic, expected with a warming
 111 climate, result from a longer thawing/summer period com-
 112 bined with increased precipitation [McCarthy *et al.*, 2001].
 113 The longer snow-free season and greater winter insulation
 114 produce secondary impacts that could cause deeper thaw of
 115 the active layer or greater melt of permanently frozen ice in
 116 glaciers and permafrost, increased biological activity, and
 117 changes in vegetative communities. Tertiary impacts arise as
 118 animals, people, and industry respond to the changing
 119 ecosystem.

120 [8] It is crucial to study the impacts of a changing climate
 121 on arctic water balances, as many processes are directly or
 122 indirectly influenced by components of the hydrological
 123 cycle, e.g., soil moisture, runoff, and evapotranspiration.
 124 However, the question if the arctic tundra will get wetter or
 125 drier is not a simple one as all the components interact with
 126 each other. In the Siberian arctic, for example, there is
 127 evidence of decreasing lake abundance despite increases in
 128 precipitation [Smith *et al.*, 2005].

129 [9] Changes to the water balance of northern wetlands are
 130 especially important because most wetlands in permafrost
 131 regions are peatlands, which may absorb or emit carbon
 132 depending on the depth of the water table [ACIA, 2004;
 133 Walsh *et al.*, 2005]. In this way, hydrologic changes will
 134 have global implications. Other important feedbacks to
 135 global warming are the albedo feedback and the weakening

of the thermohaline circulation caused by increased fresh- 136
 water flux into the Arctic Ocean. 137

138 1.3. Objective

[10] The study presented here is an application of the 139
 TopoFlow model, described in detail by Bolton [2006]. Our 140
 objective is to evaluate its capability of representing arctic 141
 hydrological processes. First, the hydrologically important 142
 processes of Imnavait Creek are described. The study then 143
 focuses on comparing the physical hydrology, measured and 144
 observed in the field, with model results. The model is 145
 executed and evaluated for its capability to reproduce the 146
 different components of the hydrological cycle. 147

149 2. Site Description

[11] The Imnavait Creek watershed is a small headwater 150
 basin of approximately 2 km², located in the northern 151
 foothills of the Brooks Range (68°30'N, 149°15'W), 152
 250 km south of the Arctic Ocean (Figure 1). The Imnavait 153
 Creek flows parallel to the Kuparuk River for 12 km before 154
 it joins the Kuparuk River that drains into the Arctic Ocean. 155
 The elevation in this area ranges from 880 m at the outlet to 156
 960 m at the southern headwaters. The area is underlain by 157
 continuous permafrost, and the topography consists of low 158
 rolling piedmont hills. Imnavait Creek has been intensively 159
 studied since 1985 by the Water and Environmental Re- 160
 search Center (WERC) at the University of Alaska, Fair- 161
 banks. This research is documented in, e.g., Hinzman *et al.* 162
 [1991, 1996], Walker *et al.* [1989], Kane *et al.* [1989, 1990, 163
 1991b], and McNamara [1997]. 164

[12] If not otherwise specified, all data reported in this 165
 section are documented by Hinzman *et al.* [1996]. In the 166
 Imnavait Creek watershed the mean annual temperature 167
 averages −7.4°C. In January (July) the average air temper- 168
 ature is −17°C (9.4°C). The annual precipitation averages 169
 340 mm, two-thirds of which falls during the summer 170
 months of June, July, and August. Most rainfall is light 171
 (82% <1 mm/h) and appears evenly distributed over the 172
 catchment. Because of the influence of wind and topogra- 173
 phy, snow distribution and snow pack volumes in the 174
 Imnavait watershed are extremely variable both in time 175
 (year to year) and space (within the watershed), ranging 176
 from a few centimeters on windswept ridgetops to more 177
 than 1 m in the valley bottom. Winter snow accumulation 178
 generally starts around mid-September. A 20-a record 179
 shows that the annual snow water equivalent (SWE) in 180
 Imnavait Creek varies from 69 to 185 mm [Berezovskaya *et* 181
al., 2005]. Snowmelt is initiated between 1 and 27 May and 182
 is completed within 6–22 d. This reveals a considerable 183
 range in timing of snowmelt initiation. The vegetation is 184
 mostly water-tolerant plants such as tussock sedges and 185
 mosses [Walker *et al.*, 1989]. Generally, with a relatively 186
 impervious barrier so close to the surface, wet conditions 187
 exist in the active layer near the surface. This provides the 188
 conditions suitable for substantial evapotranspiration during 189
 the summer thawing months [Kane *et al.*, 1989]. 190

[13] Imnavait Creek is a north draining, first-order stream. 191
 The stream is beaded, meaning that the channel connects 192
 numerous interspersed small ponds. These ponds are on the 193
 order of 2 m deep and a few meters in length and width 194
 [Kane *et al.*, 2000]; see Figure 1. 195

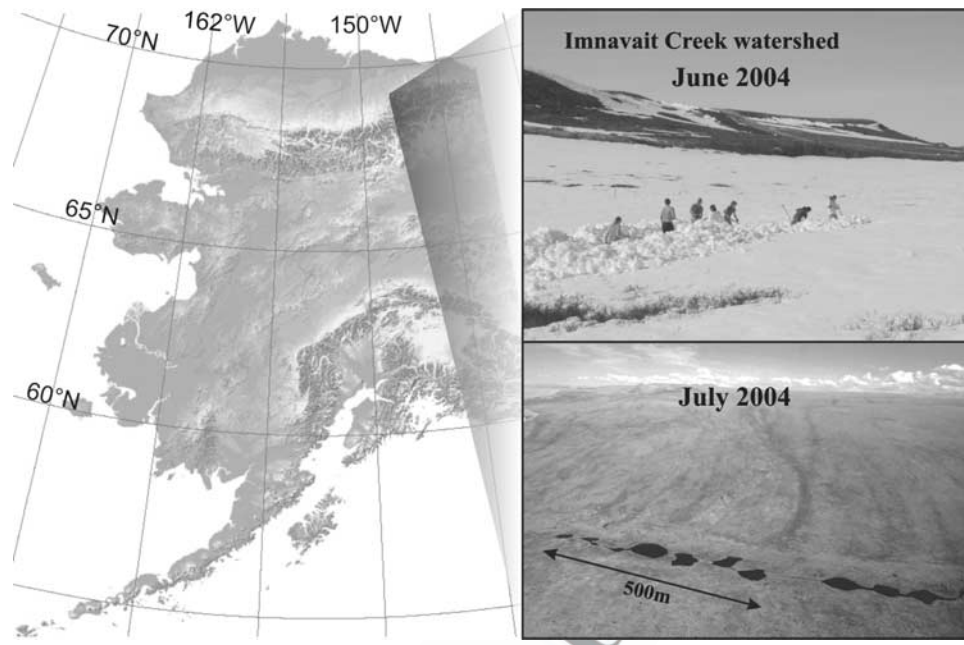


Figure 1. Map of Alaska, United States, with the location of the study area Imnavait Creek.

196 [14] The headwaters of the creek are found in a nearly
 197 level string bog, or strangmoor, with many poorly defined
 198 and interconnecting waterways [Oswood *et al.*, 1989].
 199 Along the hillslopes, small drainage channels, or water
 200 tracks, carry water off of the slopes down to the valley
 201 bottom. The water tracks can be described as shrubby
 202 corridors with a width of ~ 2 m and spaced at ~ 10 – 20 m
 203 along the hillslope. The water tracks contain a system of
 204 interconnected deepenings, or small channels of ~ 5 – 10 cm
 205 width, which are partly directed parallel to the hillslope.
 206 Here the water flow follows microtopographic features,
 207 such as tussocks and hummocks [Quinton *et al.*, 2000].
 208 Although quite obvious in aerial photographs, most of these
 209 water tracks are difficult to detect on the ground, as they are
 210 not incised [Hastings *et al.*, 1989; McNamara, 1997]. The
 211 water tracks generally take the most direct route down the
 212 slope but do not connect directly with the stream in the
 213 valley bottom. As the slope flattens out in the valley
 214 bottom, water moving down the water tracks disperses into
 215 numerous poorly defined channels and slowly makes its
 216 way over to the creek. Water moves downslope in these
 217 water tracks more rapidly than by subsurface means [Kane
 218 *et al.*, 1989].

219 [15] Runoff leaving the basin is usually confined to a
 220 period of 4 months, beginning during the snowmelt period
 221 in late May until freeze-up in September. Spring runoff is
 222 usually the dominant hydrological event of the year [Kane
 223 and Hinzman, 1988], typically producing the annual peak
 224 flow, and about 50% of the total annual runoff volume.
 225 Stream flow almost ceases after extended periods of low
 226 precipitation, whereas intense summer rainfall events pro-
 227 duce substantial stream flow. Whether runoff is produced
 228 from rainfall events during the summer is strongly related to
 229 rain intensity and duration and antecedent soil moisture
 230 conditions [Kane *et al.*, 1989]. Furthermore, the runoff
 231 response depends on the snow cover (see section 5.2), the
 232 state of the active layer, and mechanisms related to the

channel network: In a beaded stream system, small ponds 233
 act as reservoirs and can store water intermediately. This 234
 mechanism will, depending on the water level of each pond, 235
 result in a delayed hydrograph signal. Furthermore, the state 236
 of the active layer plays a pivotal role in altering runoff 237
 response. The maximum depth of thaw ranges from 25 to 238
 100 cm, severely limiting the ability of the active layer to 239
 store large quantities of groundwater. The rate of thaw is 240
 dependent upon a number of factors, such as soil properties, 241
 soil moisture and ice content, and the distribution and 242
 duration of the snow cover. As a result, the depth of the 243
 active layer and thus the soil moisture is highly variable 244
 both in space and time [Woo and Steer, 1983; Woo, 1986]. 245
 Because of the excessive water supply from snowmelt, the 246
 water table in flatter areas rises above the ground surface to 247
 generate surface flow. Spring is therefore the time when the 248
 extent of surface flow is typically at a maximum. As 249
 summer progresses, the soil moisture content is reduced 250
 by an increasing depth of thaw and a continued evapotrans- 251
 piration. This leads to a rapid depletion of the overall soil 252
 moisture content, and a nonsaturated zone develops. Occa- 253
 sional heavy rainstorms, however, can revive surface flow 254
 [Woo and Steer, 1983], and late summer and early fall 255
 rainstorms provide a recharge of soil moisture. 256

3. Models 257

3.1. Previous Studies 258

[16] At present, climate models do not represent the soil 259
 layers at high enough resolution to achieve the soil output 260
 needed to assess changes in permafrost distribution and 261
 active layer characteristics. The need for additional detail is 262
 particularly great for areas with thin or discontinuous 263
 permafrost [Walsh *et al.*, 2005]. Furthermore, the majority 264
 of land surface models have been primarily designed for 265
 lower latitudes and as such are not capable of realistically 266
 simulating the physical processes operating in the extreme 267

268 climate of the arctic. However, increasing efforts have been
269 made to adequately model arctic environments over the last
270 2 decades. Several modeling studies with varying focuses
271 have been applied to the Imnavait Creek watershed, where
272 field data from multiple-year studies are available.

273 [17] *Hinzman and Kane* [1992] studied the potential
274 hydrological response during a period of global warming
275 using the HBV model. The original version of this model
276 was developed in 1975 by the Swedish Meteorological and
277 Hydrological Institute as a conceptual runoff model and
278 modified for cold regions use by *Bergström* [1976]. It can
279 be described as a reservoir-type model with routines for
280 snowmelt, soil moisture accounting, control of surface and
281 subsurface hillslope runoff response, and a transformation
282 function to handle stream routing. The model input data are
283 observations of air temperature, precipitation, and estimates
284 of evapotranspiration. Model outputs are snowmelt runoff
285 and the entire summer runoff response. Despite of the good
286 congruence of measured and simulated hydrographs the
287 authors report several shortcomings: First, the lack of
288 physically based routines queries its capability of evaluating
289 future changes. Second, the prediction capability could be
290 improved by incorporating the redistribution of snow by
291 winds and the retardation of runoff by snow damming
292 [*Hinzman and Kane*, 1992].

293 [18] Another model was applied to the same study area by
294 *Stieglitz et al.* [1999]. The simple land surface model
295 TOPMODEL was used to explore the dynamics of the
296 hydrologic cycle operating in arctic tundra regions. The
297 model accounts for the topographic control of surface
298 hydrology, ground thermal processes, and snow physics.
299 This approach relies only on the statistics of the topography
300 rather than its details. This has the advantage of being
301 computationally inexpensive and compatible with the large
302 spatial scales of today's climate models. However, the
303 authors report several deficiencies, such as that the model
304 performance in temperate watersheds is superior to that for
305 arctic watersheds. This is attributed to the neglect of snow
306 heterogeneity, which poses a real obstacle toward applica-
307 tion on an arctic-wide basis. Furthermore, the representation
308 of a seasonally changing connectivity of waterways (e.g. the
309 beaded stream system) is seen to be difficult on a statistical
310 base. As such, TOPMODEL is capable of simulating the
311 overall balances, but shortcomings exist in the hydrograph
312 simulation and soil moisture heterogeneity with high tem-
313 peral resolution.

314 [19] A third modeling study with an application to Imna-
315 vait Creek is presented by *Zhang et al.* [2000]. Here a
316 process-based, spatially distributed hydrological model is
317 developed to quantitatively simulate the energy and mass
318 transfer processes and their interactions within arctic
319 regions (Arctic Hydrological and Thermal Model
320 (ARHYTHM)). The model is the first of this kind for areas
321 of continuous permafrost and consists of two parts: the
322 delineation of the watershed drainage network and the
323 simulation of hydrological processes. The last include
324 energy-related processes such as snowmelt, ground thaw-
325 ing, and evapotranspiration. The model simulates the dy-
326 namic interactions of each of these processes and can
327 predict spatially distributed snowmelt, soil moisture, and
328 evapotranspiration over a watershed as well as discharge in
329 any specified channels. Results from the application of this

model demonstrate that spatially distributed models have 330
the potential for improving our understanding of hydrology 331
for certain settings. Nevertheless, the authors point out that 332
an algorithm for snow damming, the usage of a higher 333
resolution, and a better data collection network could 334
improve the model results. Furthermore, the use of triangu- 335
lar elements makes it difficult to compare simulation results 336
with other (e.g., remotely sensed) data sets. 337

[20] From former studies it becomes evident that topog- 338
raphy plays a crucial role in the development of soil 339
moisture heterogeneity. The fact that the impacts of this 340
heterogeneity on surface water and energy fluxes are critical 341
and perhaps overwhelming [*Stieglitz et al.*, 1999] leads to 342
the conclusion that the representation of topographic fea- 343
tures in a model cannot be neglected. Furthermore, there 344
exist problems in the current models to handle the rapidly 345
changing thermal (permafrost versus nonpermafrost and 346
active layer development) and hydraulic (hydraulic con- 347
ductivity and storage capacity) conditions typical of the 348
(sub)arctic regime [*Bolton et al.*, 2000]. 349

3.2. TopoFlow 350

[21] TopoFlow is a spatially distributed, process-based 351
hydrological model, primarily designed for arctic and sub- 352
arctic watersheds. TopoFlow is primarily based upon the 353
merger of the ARHYTHM model [*Hinzman et al.*, 1995] 354
and a D8-based rainfall-runoff model. Structurally, the most 355
significant differences between the ARHYTHM and Topo- 356
Flow models are the incorporation of rectangular elements 357
and flow routing using the D8 method. In the D8 method, 358
horizontal water fluxes occur from one element to one of the 359
eight adjacent elements in the direction of the steepest slope 360
[*O'Callaghan and Mark*, 1984]. The model domain is 361
defined by a rectangular, regular network DEM that encom- 362
passes the catchment area. Each TopoFlow element has 363
dimensions of the DEM pixel (x and y directions) with up to 364
ten user-specified layers of variable thickness in the z 365
direction. On the basis of the conservation of mass princi- 366
pal, TopoFlow simulates major processes of the water 367
balance (precipitation, snowmelt, evapotranspiration, 368
groundwater flow, and overland/channel flow) as well as 369
some storage processes (snow accumulation and infiltration/ 370
percolation). Most of these hydrologic processes are formu- 371
lated in the exact manner as the ARHYTHM model and are 372
well documented by *Zhang et al.* [2000]. Yet important 373
improvements have been made in the process simulation 374
component of the model. These improvements include 375
expansion of the methods available to simulate the infiltra- 376
tion and channel flow processes, the ability to handle a 377
variety of input variable formats, and a user-friendly inter- 378
face. A detailed description of the model structure and the 379
additional methods incorporated into TopoFlow can be 380
found in the work of *Bolton* [2006]. 381

[22] The development of soil moisture heterogeneity and 382
its correct reproduction in models is crucial for the evalu- 383
ation of its impacts on surface water and energy fluxes 384
[*Boike et al.*, 1998]. TopoFlow addresses these issues 385
through (1) its spatial distribution that explicitly models 386
the movement of water from element to element; (2) by the 387
implementation of physical routines that are unique in cold 388
regions; (3) by providing user-friendly preprocessing tools 389
that aid in handling the spatial variability, such as the 390

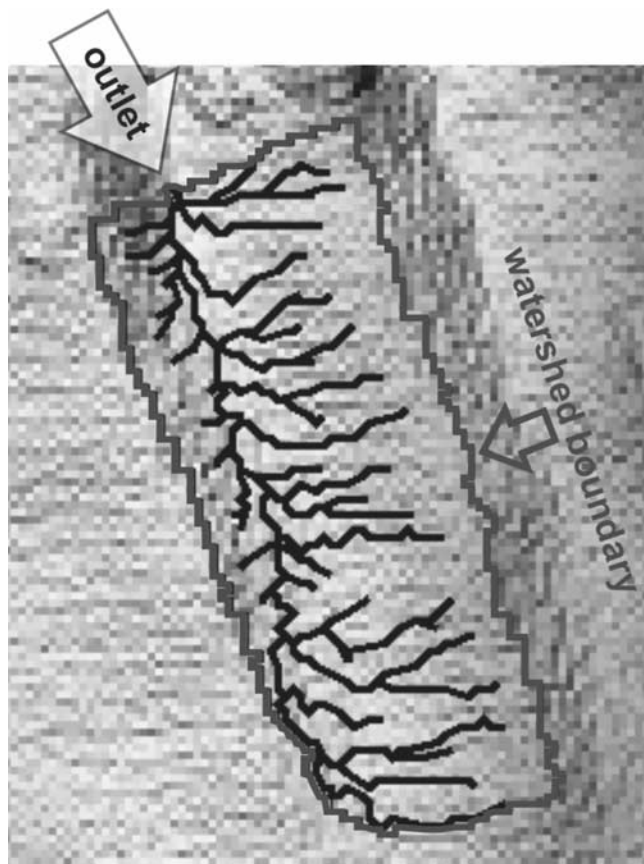


Figure 2. Digital Elevation Model of the Innavait Creek watershed, its channel network, and watershed boundaries.

391 distribution of permafrost versus nonpermafrost, the active
 392 layer depth, and the snow pack distribution; and (4) by
 393 providing a flexible structure that allows the user deal with
 394 different data types or the lack of measured parameters.

395 [23] The hydrological simulation is initiated some hours
 396 prior to snowmelt with the end of winter snow pack
 397 distribution used as input. TopoFlow supports the degree
 398 day and the energy balance method for snowmelt. For
 399 evapotranspiration, two methods are provided to account
 400 for different availability of input data: the physically based
 401 energy balance and the semiempirical Priestley-Taylor ap-
 402 proach. TopoFlow allows the spatial distribution of impor-
 403 tant parameters, such as meteorological variables or
 404 coefficients, soil moisture content, soil parameters, and
 405 snow pack distribution.

406 [24] At the time of this study an instantaneous infiltration
 407 method was available, and the three different flow processes
 408 (channel flow, overland flow, and subsurface flow in the
 409 shallow active layer) were incorporated into the model with
 410 Darcy's law and Manning's equation [Schramm, 2005].
 411 Further improvements of the infiltration and percolation
 412 process, such as the finite difference solution of the
 413 Richards equation, Green-Ampt, and Smith-Parlange, have
 414 recently been incorporated [Bolton, 2006] (TopoFlow Web
 415 site, <http://instaar.colorado.edu/topoflow/>).

416 [25] The active layer starts thawing after snowmelt, con-
 417 tinues to thaw during the summer, and reaches its maximum
 418 thickness in autumn. Therefore the soil depth in Darcy's

equation potentially changes with each time step. Soil 419
 moisture capacities for each soil layer also change, because 420
 they are related to the soil depth. As the hydraulic conduc- 421
 tivity is different for the frozen and the unfrozen soil, flow 422
 rates in the frozen layers differ significantly from those in 423
 the unfrozen soil. The thawing of the active layer is 424
 currently incorporated by a simple square root of time 425
 function [Hinzman *et al.*, 1990]. 426

[26] For the overland and channel flow, Manning's formula 427
 is used, where the roughness parameter, the shape of 428
 the cross section, and the channel width can be specified by 429
 the user for each stream order. 430

4. Model Application 432

4.1. Digital Elevation Model (DEM) 433

[27] A DEM with a pixel size of 25×25 m is used in this 434
 study. In order to create the input files necessary for Topo- 435
 Flow simulations, the hydrological software package River- 436
 Tools is used in this study. RiverTools defines 437
 computationally the watershed area that contributes to a 438
 user-specified element. In this study a watershed area of 439
 1.9 km^2 was calculated. This is in good agreement with the 440
 manual delineation of 2.2 km^2 , taking into account that the 441
 headwaters are complex topographically, i.e., a very flat 442
 area, and therefore the southern watershed boundary is 443
 difficult to determine visually and/or by way of calculation. 444
 Figure 2 depicts the DEM of the Innavait Creek watershed, 445
 its channel network, and watershed boundaries. 446

[28] The DEM is used in RiverTools to generate several 447
 files that are needed to extract information for a river 448
 network. The flow grid indicates the direction in which 449
 water would flow away from the corresponding pixel in the 450
 DEM. Here RiverTools provides special algorithms to 451
 determine the flow direction in flat areas that are common 452
 in the arctic tundra. Furthermore, a RiverTools treefile is 453
 derived from the flow grid. This vector-formatted file stores 454
 data for the basin such as contributing area and relief. These 455
 attributes are stored for every element in a given basin. 456

[29] In order to differentiate where channel flow and 457
 overland flow processes occur, the simulated channel net- 458
 work is compared to the physical system. Elements with a 459
 stream order of less than 3 are considered to be overland 460
 flow, and those ≥ 3 are locations where channel flow is 461
 present. Considering the water tracks (described in section 2) 462
 to be channels, the simulated river network compares well 463
 with the channel structure that is visible in aerial pictures. 464
 Finally, grids of upstream areas, downstream slopes, and 465
 Horton-Strahler order are produced with RiverTools for 466
 further use with TopoFlow. 467

4.2. Input Data 468

[30] Various research projects on the North Slope of 469
 Alaska have, since the mid 1980s, resulted in the establish- 470
 ment of several unmanned meteorological and research sites 471
 on a north-south transect located along the Dalton High- 472
 way. The measurement program is maintained by WERC, 473
 and data are available on the WERC Web site ([http://](http://www.uaf.edu/water) 474
www.uaf.edu/water). In the Innavait Creek basin there are 475
 four main sites where data collection takes place: Innavait 476
 basin ($68^{\circ}36'N$, $149^{\circ}18'W$, 937 m); Innavait ridge 477
 ($68^{\circ}37'N$, $149^{\circ}19'W$, 880 m); Innavait valley ($68^{\circ}37'N$, 478

t1.1 **Table 1.** Soil Parameters of Imnavait Creek Used as Model Input^a

t1.2	Soil Layer Depth, cm	Porosity, %	Hydraulic Conductivity, 10 ⁴ m/s
t1.3	0–10	0.88	1.50
t1.4	10–20	0.63	0.35
t1.5	20–30	0.50	0.35
t1.6	30–40	0.48	0.10
t1.7	40–permafrost table	0.40	0.10

t1.8 ^aData based on *Hinzman et al.* [1991].

479 149°19'W, 876 m); and Imnavait flume station (68°37'N,
480 149°19'W, 881 m). Compared with other arctic research
481 basins an immense amount of data has been collected in the
482 Imnavait Creek watershed. Most of the major processes
483 have been monitored continuously since 1985 [*Kane et al.*,
484 2004].

485 [31] Measurements collected from 2001 to 2003 are used
486 in this study. Soil data from former studies complete the
487 data collection. Sensors for air temperature, air pressure,
488 wind speed, wind direction, relative humidity, radiation, soil
489 temperature, and precipitation measure automatically. Ex-
490 cept for the radiation measurements (March to September)
491 the recording takes place throughout the year. All meteorolo-
492 gical data used in this study are conducted at the Imnavait
493 basin site. Liquid precipitation is measured using a tipping
494 bucket rain gage equipped with a windshield. The threshold
495 sensitivity of the tipping basket is 1 mm of rain, and the
496 undercatch is estimated to be 5% (D. L. Kane, personal
497 communication, 2007). The precipitation data used in this
498 study have not been corrected to consider the undercatch.
499 Stream discharge is estimated from stage data using a stage-
500 discharge relationship. Discharge is measured from the
501 beginning of the snowmelt until freeze-up. In July 2004,
502 measurements were carried out at Imnavait Creek to obtain
503 values for Manning's roughness parameter used in the
504 modeling. These measurements were taken at two locations
505 close to the flume station with both sections being several
506 meters in length. An average value of 0.01 s/m^{1/3} was
507 determined, but is likely to be underestimated due to
508 measurement restrictions [*Schramm*, 2005].

509 [32] The shallow soils consist of a layer of about 10 cm of
510 organic material over 5–10 cm of partially decomposed
511 organic matter mixed with silt which overlays the glacial
512 till. Generally, there is a thicker organic layer in the valley
513 bottom (~50 cm) than on the ridges (~10 cm). The soil
514 parameters used in this study are based on a representative
515 profile measured by *Hinzman et al.* [1991].

516 [33] Values for the annual active layer depth are based on
517 Circumpolar Active Layer Monitoring (CALM) measure-
518 ments ([http://www.geography.uc.edu/~kenhinke/CALM/](http://www.geography.uc.edu/~kenhinke/CALM/sites.html)
519 [sites.html](http://www.geography.uc.edu/~kenhinke/CALM/sites.html)). The depth is measured each summer at the latest
520 possible date prior to the annual freeze-up. The instrument
521 used is a metal rod that is pushed vertically into the soil to
522 the depth at which ice-bonded soil provides firm resistance.
523 This determines the maximum depth of thaw (MDT). For
524 Imnavait Creek, approximately 120 measurements are taken
525 and averaged each year.

526 [34] The position of the water table used in this study is
527 interpolated from measurements of volumetric soil moisture
528 content made using time domain reflectometry sensors at
529 seven depths within the soil profile at three sites located on
530 the west facing slope of the watershed [*Overduin*, 2005].

[35] The SWE is measured late each spring just prior to 531
snowmelt. To provide SWE data, snow depths are combined 532
with pit studies to measure snow density, temperature, and 533
hardness profile [*Reynolds and Tenhunen*, 1996]. The 534
measurements are conducted along a valley transect, ap- 535
proximately in the middle of the basin. Each reported value 536
is an average of at least 10 measurements [*Kane et al.*, 537
2001]. 538

4.3. Calibration/Parameterization 539

[36] To simulate snowmelt, two methods are used to 540
compare their ability to reproduce the snow pack ablation: 541
the degree day method (model generated) and the energy 542
balance method (calculated separately, as this method was 543
not available at the time of this study). Concerning the 544
degree day method, two parameters mainly determine the 545
simulated snowmelt: the melt factor C_0 and the threshold 546
value of the air temperature T_0 . In this study a value of 547
2.3 mm/d °C for C_0 , is found to produce the best results. T_0 548
is set to -1.2°C . When using the energy balance method for 549
snowmelt (and later evapotranspiration), the average surface 550
roughness length z_0 needs to be evaluated. In this study a 551
constant value of 0.0013 m (0.02 m) for surface roughness 552
length is used for the simulation of the melt period (evapo- 553
transpiration during summer). These values were deter- 554
mined by *Hinzman et al.* [1993]. Standard values are used 555
for latent heat of fusion ($3.34 \cdot 10^6$ J/kg), latent heat of 556
vaporization ($2.48 \cdot 10^6$ J/kg), water density (1000 kg/m³), 557
specific heat of air (1005.7 J/kg °C), density of air 558
(1.2614 kg/m³), and heat capacity of snow (2090 J/kg °C). 559

[37] Two methods are used in this study to calculate the 560
amounts of water lost by evapotranspiration: the Priestley- 561
Taylor method (model generated) and the energy balance 562
method (calculated separately as this method was not 563
available at the time of this study). For the Priestley-Taylor 564
method the parameter α_{PT} , an empirical parameter, relates 565
actual to equilibrium evaporation [*Priestley and Taylor*, 566
1972; *Rouse et al.*, 1977; *Mendez et al.*, 1998; *Kane et* 567
al., 1990]. In this study its calibration is based on the best 568
alignment with the results obtained by the energy balance 569
method, as this approach is physically based. Thus the best 570
 α_{PT} is determined to be 0.95. This value is used as an 571
average for the entire watershed. For the thermal heat 572
conductivity a value of 0.45 W/m °C was used that was 573
determined through field measurements [*Hinzman et al.*, 574
1991]. 575

[38] For the energy balance method, evapotranspiration is 576
calculated as described by *Zhang et al.* [2000]. When this 577
study was conducted, the energy balance methods (snow 578
melt and evapotranspiration) were not incorporated into the 579
model yet, and thus no spatially distributed variables could 580
be used. This would have been possible for the degree day 581
method and the Priestley-Taylor method, but was not done 582
since the aim was to compare these methods to the results of 583
the energy balance approach. 584

[39] The assignment of soil parameters to the horizontal 585
soil layers (see Table 1) is based on studies by *Hinzman et* 586
al. [1991] and the application of ARHYTHM to the same 587
study site by *Zhang et al.* [2000]. When this study was 588
conducted, a physically based representation of the active 589
layer thawing process was not yet available. Instead, input 590
files with changing hydraulic conductivities are used to 591

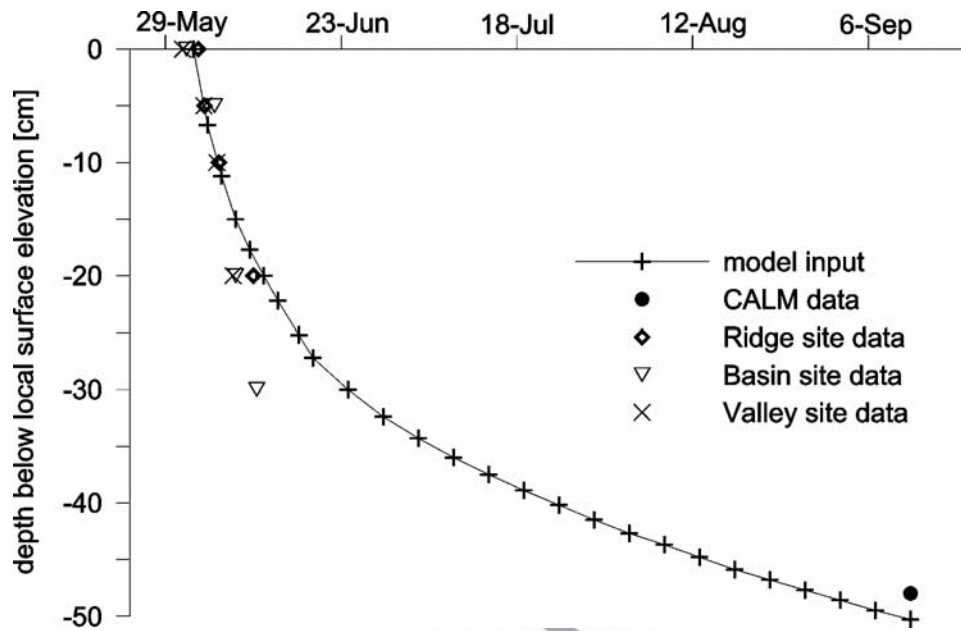


Figure 3. Thaw depth of the active layer 2001 used as a model input ($\alpha_{TD} = 0.068$ during snow melt period 25 May to 14 June; $\alpha_{TD} = 0.032$ during summer period 15 June to 13 September), determined from soil temperature measurements at the ridge, basin, and valley sites and from Circumpolar Active Layer Monitoring (CALM) grid measurements (average value).

592 account for the thawing of the soil. The soil is divided into
 593 layers of 10 cm, down to the maximum depth of thaw
 594 (MDT). During the course of the summer the thawing of the
 595 soil progresses and hydraulic conductivities are gradually
 596 (layer by layer) changed from frozen to unfrozen. The
 597 gradient controlling how the thaw depth evolves with time
 598 is determined by the α_{TD} value. The α_{TD} value is calibrated
 599 such that (1) during the initial thawing the input files match
 600 soil temperature recordings, and (2) at the end of the season
 601 the MDT matches the CALM grid measurements. Figure 3
 602 shows the evolution of a gradually thawing active layer
 603 when used as a model input for 2001 and corresponding
 604 values obtained from measurements.

605 [40] When this study was conducted, the model did not
 606 allow the use of spatially distributed hydraulic conductivities
 607 and the thawing of the soil representing conductivities
 608 at the same time. In the case of a whole summer runoff
 609 simulation the thawing of the soil is an important factor and
 610 cannot be neglected. Thus the simulations are done on
 611 spatially homogeneous soil parameters.

612 [41] In this model, overland flow occurs when the water
 613 table rises above the surface. It is assumed that all of the
 614 water from precipitation or snowmelt is instantaneously
 615 infiltrated, meaning that the percolation time from the
 616 surface to the water table is neglected. The water content
 617 in each element may change with each time step, and the
 618 total storage capacity of each element may also increase or
 619 decrease as the active layer thaws.

620 [42] The crucial factor in determining overland and chan-
 621 nel flow is the roughness parameter in Manning’s equation
 622 [Zhang *et al.*, 2000]. In this study the coefficient is
 623 subjected to calibration within the range of values obtained
 624 from field measurements and literature [Maidment, 1992;
 625 Emmett, 1970]. For channel flow the channel bed width

must be specified as well. Table 2 contains the corresponding
 values for each stream channel order.

5. Results

5.1. Water Balances 2001–2003

[43] The years 2001 to 2003 differ considerably in terms
 of hydrological and meteorological components. For the
 water balances (Figure 4), measured data are used for the
 rain, snow, and discharge components. Evapotranspiration
 is calculated with the energy balance method. The storage
 equals the residual term of the input (rain and snow) minus
 the output (discharge and evapotranspiration). Thus the
 storage term also includes the sum of errors caused by
 measurement uncertainties.

[44] In 2001 to 2003 the mean annual precipitation
 amounts to 337 mm, 520 mm, and 479 mm, respectively.
 Runoff accounts for 54%, 60%, and 67% of the water
 budget. The total amount of evapotranspiration is 48%,
 42%, and 28% of the water budget. In each year the winter
 snow pack is a major source that adds water to the system.
 For the years of this study it accounts to 33–41% of the
 total amount of water added. A remarkable snow fall of
 126 mm occurred in August 2002. The storage term,

Table 2. Overland and Channel Flow Parameters Used as Model Input^a

	Manning’s Roughness Parameter, s/m ^{1/3}	Channel Bed Width, cm	
Overland flow	0.30	-	t2.3
Water tracks	0.15	5	t2.4
Stream order 2	0.10	15	t2.5
Stream order 1	0.07	40	t2.6

^aData determined by field measurements and calibration.

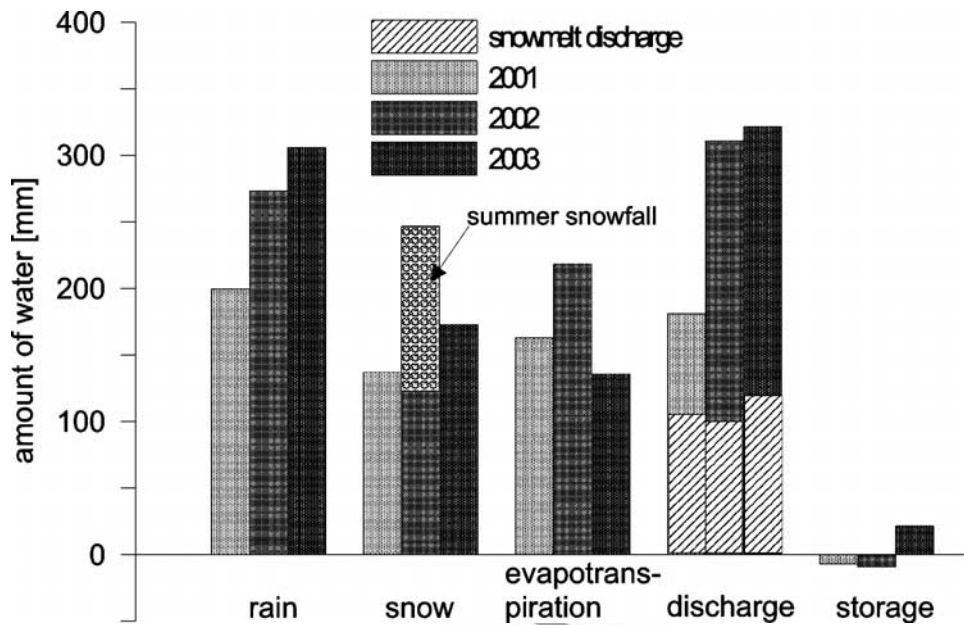


Figure 4. Water balance components for 2001–2003. Rain, snow, and discharge are based on measured data. Evapotranspiration is calculated using the energy balance method.

649 calculated as the residual term, shows little differences from
 650 year to year. Whereas in 2001 and 2002 the change in
 651 storage is slightly negative, there is a gain of 21 mm at the
 652 end of 2003.

653 [45] In the Innavait watershed, 2001 represents an
 654 average year in most hydrologic components, whereas
 655 2002 and 2003 show special characteristics that differ
 656 from mean values. 2003 is a wet year with continuously
 657 high precipitation, little evapotranspiration, high dis-
 658 charge, and a gain in soil moisture. Conversely, 2002 is
 659 characterized by the unusual summer snow fall and a
 660 high amount of evapotranspiration.

[46] Figure 5 shows the measured cumulative discharges
 661 of all years from the beginning of snowmelt until freeze-up,
 662 revealing distinct differences each year. The early onset of
 663 snowmelt in 2002 causes a considerably earlier start of
 664 discharge. Whereas in 2001 and 2003 the melt discharge is
 665 the highest discharge of the year, the peak discharge in 2002
 666 originates from a snow/rain event in late summer.
 667

[47] The influence of the antecedent soil moisture con-
 668 ditions on the runoff signal has been stated in section 2. This
 669 role is evident in each year of this study. For example, in
 670 2002 the highest storm event of 9.3 mm/h recorded at
 671 21 July results in a barely noticeable rise in runoff, after a
 672

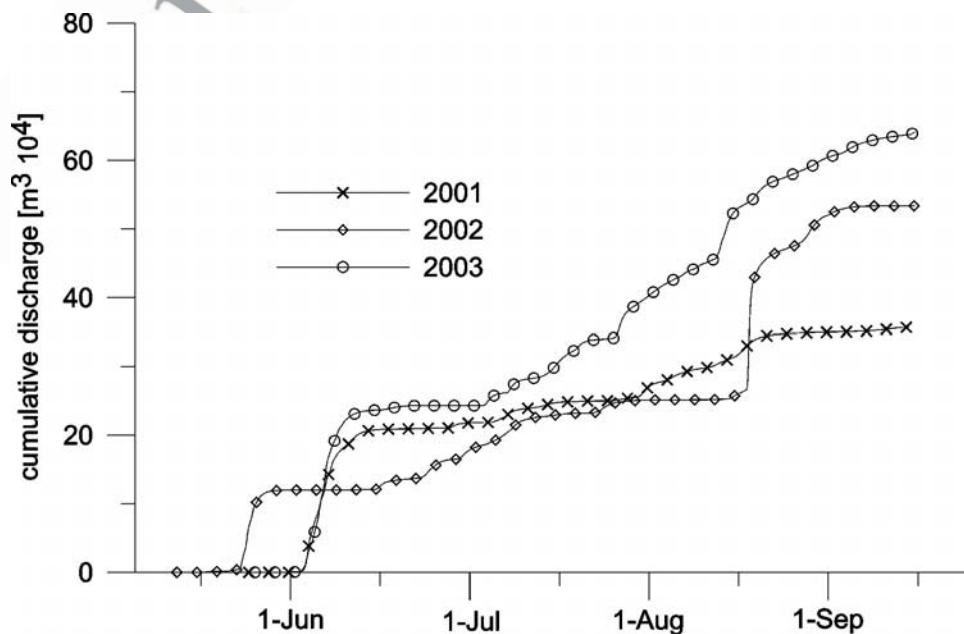


Figure 5. Measured cumulative discharges at Innavait Flume station 2001–2003.

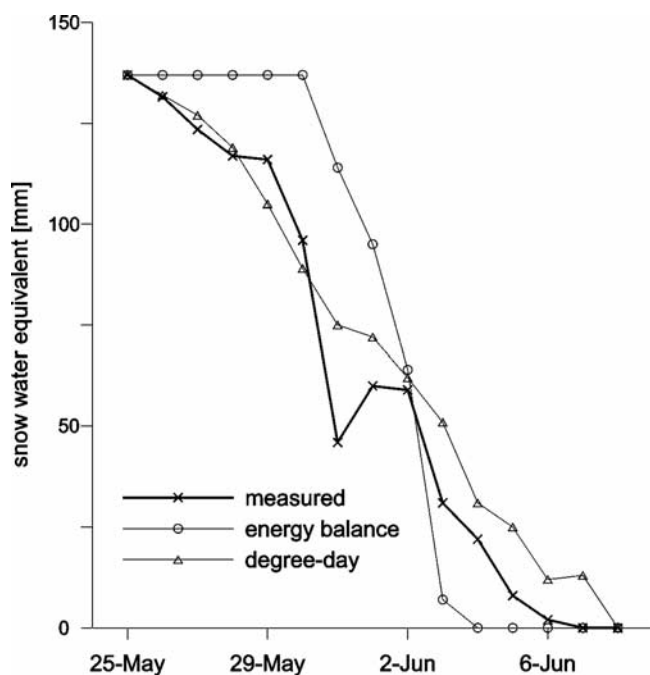


Figure 6. Measured and simulated snow ablation 2001.

673 7-h delay. Instead, a following rain event of 7 mm/h the next
 674 day generates a rise in discharge that exceeds the previous
 675 one by 3 times in peak and total amount. Also, the highest
 676 discharge on record with about 3.7 m³/s is generated by a
 677 precipitation of 6 mm/h about 5 h earlier. In the first case a
 678 dry period of 7 d preceded the heavy rain event, whereas in
 679 the last two cases, precipitation was recorded previously.

680 [48] The discharge recorded at the end of the summer
 681 season 2003 shows an interesting feature not uncommon in
 682 arctic environments: At the time where the last peak occurs,
 683 freeze-up has already started, and surface temperatures
 684 show negative values for approximately 6 d. In addition,
 685 the last rain event that could have generated runoff is
 686 recorded 7 d prior to the peak in discharge. An explanation
 687 (R. E. Gieck, personal communication, 2004) for the
 688 occurring runoff could be that frazil ice and snow in the
 689 channel had blocked the outflow of one of the ponds
 690 upstream. When the ice dam broke, a small flood surge
 691 passed through the flume.

692 5.2. Modeling Results

693 5.2.1. Snowmelt

694 [49] In 2001 the snow pack ablated within 13 d. The
 695 initial SWE is obtained from snow survey measurements
 696 done prior to ablation. An average value is used for the
 697 entire watershed.

698 [50] Two methods, the degree day method (SM-DD) and
 699 the energy balance approach (SM-EB), are used to deter-
 700 mine the snow pack ablation. SM-DD is used in the model
 701 simulation, whereas SM-EB is calculated separately.
 702 Figure 6 shows the simulated and the measured ablation
 703 curves for 2001. SM-DD achieves a better congruence than
 704 the energy balance method. Using the energy balance
 705 method, the onset of melt is delayed by 5 d, but completed
 706 earlier than measured. In the degree day method, the onset

of snowmelt coincides exactly with the real onset, but the
 end of snowmelt is delayed.

[51] The discrepancy in congruence of the simulation and
 the recording could partly be due to the fact that field
 measurements are made daily in the morning, whereas both
 melt algorithms operate at hourly time steps. In addition, the
 pronounced spatial variability of the snow pack was stated
 previously, and other studies emphasize that the considera-
 tion of snow cover heterogeneity over complex arctic
 terrain provides a better representation of the end-of-winter
 snow water equivalent and an improved simulation of the
 timing and amount of water discharge due to snowmelt.

5.2.2. Discharge

[52] Measured versus simulated hydrographs for the year
 2001, and the corresponding cumulative discharges, are
 depicted in Figure 7. It should be noted that because of
 the model configuration the simulation is split into snow-
 melt and summer period. The initial water table at the
 beginning of the summer simulation is set to the simulated
 height of the water table at the end of the snowmelt period.

[53] The diurnal fluctuations during the melt period,
 reflecting the influence of daily snowmelt cycles, are
 obvious in both, measured and simulated hydrographs.
 The onset of simulated discharge after snow melt occurs
 7 d earlier than the measured one. Whereas this difference to
 the measured hydrograph is obvious, the total volume of
 melt discharge is very close to reality. The deviation in onset
 occurs because an algorithm for snow damming has not
 been incorporated into the model. Snow, redistributed by
 wind, accumulates in water tracks and valley bottoms,
 where melt water collects. The water seeps through the
 snow until it reaches a degree of saturation where both snow
 and melt water start to move, cutting a channel through the
 snow pack. Kane *et al.* [1989] found from measurements in
 the Innvait watershed that the reduction of the snow water
 equivalent reaches up to 80% before stream runoff starts.

[54] Another explanation for the discrepancy between
 modeled and measured hydrograph could be the spatial
 variability of the snow pack. In this study an average value
 for initial SWE is used as an input, whereas in reality the
 variability of snow distribution with topography is pro-
 nounced [Kane *et al.*, 1991b; Hinzman *et al.*, 1996].

[55] During the summer runoff period the predicted
 cumulative discharge agrees well with the measured dis-
 charge volume. The simulated hydrograph caused by sum-
 mer storm events shows some deviation from the
 recordings. For most rain events the simulated discharge
 leads measured data. Measured peak discharges are usually
 lower and have a longer recession time. The Nash-Sutcliffe
 coefficient for a weekly average is 0.64. An explanation for
 this discrepancy could be the beaded stream system, where
 small ponds act as reservoirs and store water intermediately,
 resulting in an attenuated hydrograph signal.

[56] Results indicate that the model performs well in the
 quantitative reproduction of the streamflow processes, but
 could be refined further in the timing of small-scale, short-
 term processes (see section 5.3).

5.2.3. Evapotranspiration

[57] Cumulative evapotranspiration and daily evapotrans-
 piration rates for 2001 are shown in Figure 8. Evapotrans-
 piration is only determined during the summer season.
 Priestley-Taylor (ET-PT) values are calculated by the

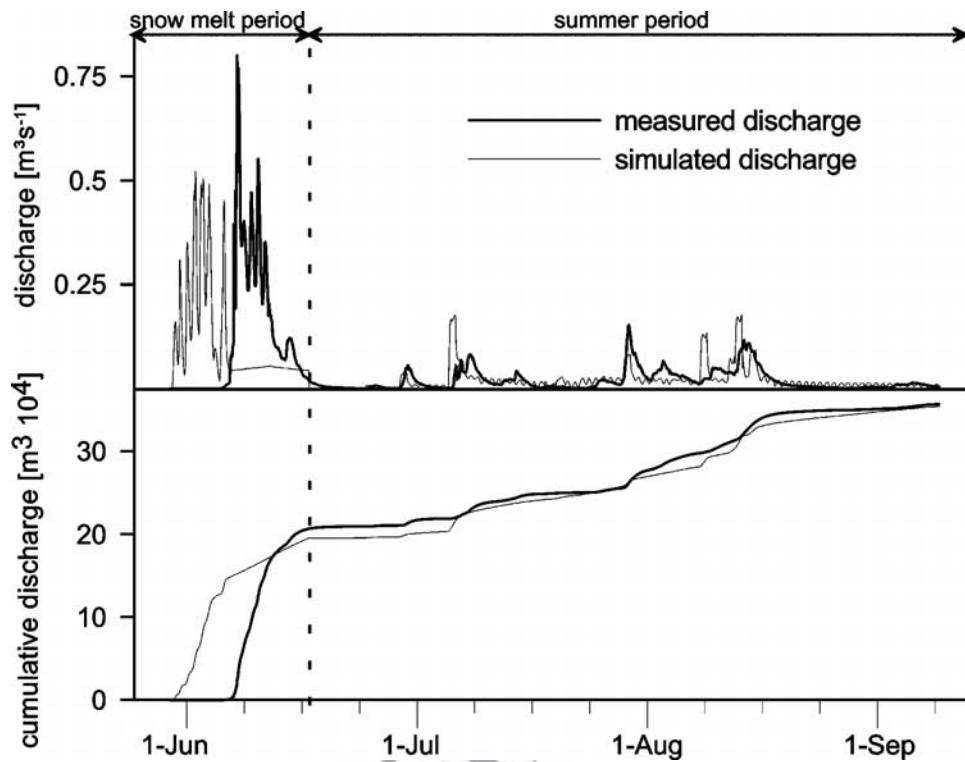


Figure 7. Measured and simulated discharge 2001.

769 model, whereas energy balance (ET-EB) calculations are
770 done externally.

771 [58] In the total amount, ET-PT agrees well with the
772 results of ET-EB. Figure 8 also illustrates the differences
773 between ET-PT and ET-EB. Whereas fluctuations are pro-
774 nounced in ET-EB, and fluxes are occasionally directed
775 downward, ET-PT shows a steady rise without major
776 fluctuations. This is due to the fact that both methods differ
777 in the representation of the ventilation term, including the
778 deficit in saturation and the wind component. ET-EB

obtains this term from measurements, whereas in ET-PT 779
780 this term is replaced by a constant. The ET-EB calculation
781 shows the highest flux rates in early summer when both
782 energy and water are relatively abundant.

5.2.4. Water Table 783

[59] Simulation results are compared with the measured 784
785 water table height during summer 2003 at a water track site
786 within the watershed (Figure 9). The year 2003 was chosen
787 for this simulation, because measurements were available
788 only for this period. Qualitatively, the simulation shows the

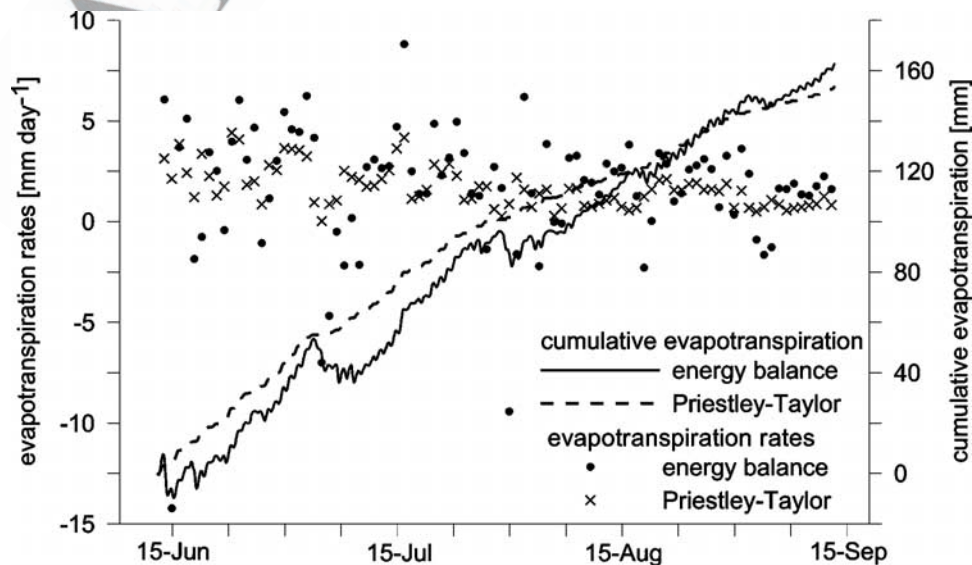


Figure 8. Cumulative hourly evapotranspiration 2001 and daily evapotranspiration rates 2001. The $\alpha_{PT} = 0.95$ in the Priestley-Taylor calculation.

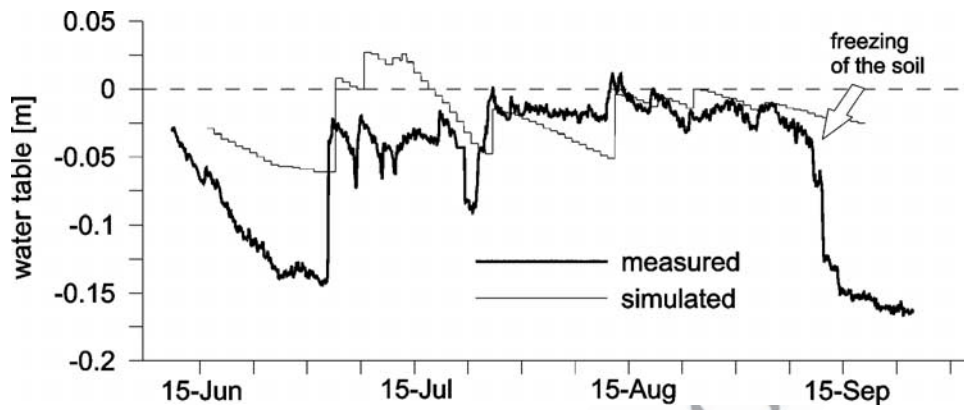


Figure 9. Comparison of simulated and measured water tables during the summer 2003 at a water track. Unit is water table (meters) relative to the local surface elevation. Refreezing of the soil results in the rapid decline of the measured water table in September.

789 same trends as the measurement. The sudden rises in the
 790 simulated water table are due to the instantaneous infiltration
 791 routine, where water percolation through the soil is
 792 neglected. The rapid decline in measured water table in
 793 September is caused by freezing of the soil. This process is
 794 not considered in the model simulations.

795 **5.3. Model Sensitivity Toward Change in Parameters**

796 [60] Figure 10a gives evidence of the influence of the
 797 MDT on total discharge. The importance of MDT is
 798 twofold: First, MDT has (in the current state of TopoFlow)
 799 to be given as input and thus underlies the uncertainties of

measurements. For example, *Boike et al.* [1998] found that
 800 ground thaw depths determined using the probe method
 801 deviated considerably from the thaw depths determined by
 802 soil temperatures during the period when the active layer
 803 was dry. This is explained by a greater case of penetration of
 804 the frost probe when the active layer is saturated. Second, a
 805 simulation with increased MDT can reveal the runoff
 806 response to an increased melting of ground ice. In this
 807 study an increased MDT of 70 cm (compared to the normal
 808 case of 50 cm) is used in the summer simulation 2001.

[61] Figure 10b gives evidence of the importance of the
 810 initial water table height. It should be noted that only the
 811

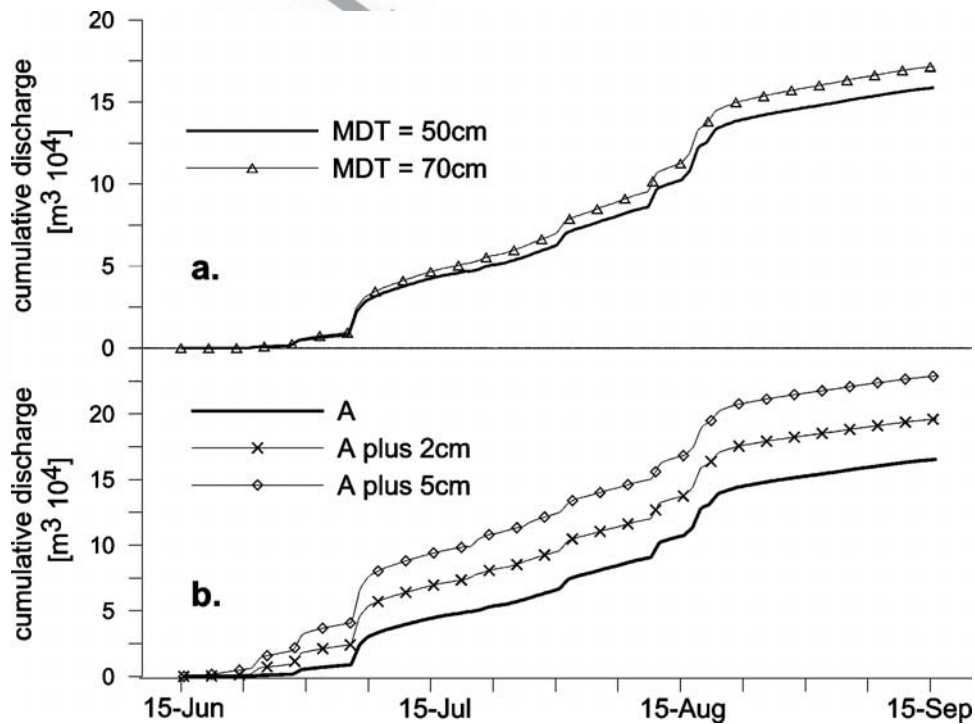


Figure 10. (a) Simulated discharge 2001 using different active layer depths. Maximum depth of thaw (MDT) is 50 cm in the normal 2001 simulation and was lowered to 70 cm for sensitivity studies. (b) Simulated discharge 2001 using different initial water table heights. Case A represents the normal water table height of the 2001 simulation. In the other simulations the water table height was raised by 2 cm and 5 cm, respectively.

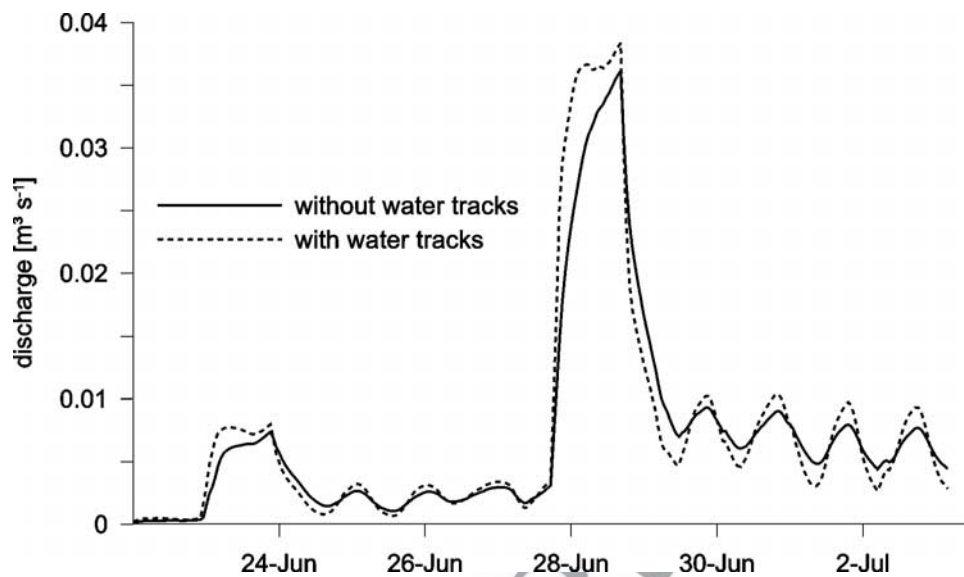


Figure 11. Simulated discharge 2001 illustrating the influence of water tracks. Solid line shows the normal 2001 simulation. Dashed line represents the discharge in a simulation where the water tracks were leveled to the adjacent surface elevation.

812 initial state of the water table height is given as an input,
813 whereas its further evolution is calculated by the model.
814 Here a small increase of 2 cm (5 cm), compared to the
815 normal water table height (case A) causes an increase of
816 19% (38%) in the total amount of discharge. On the one
817 hand, the influence of the antecedent soil water content on
818 total discharge is characteristic for arctic watersheds where
819 subsurface processes are limited to the shallow active layer.
820 On the other hand, one should be aware of this sensitivity
821 when calibrating the model.

822 [62] Figure 11 shows simulated hydrographs where the
823 effect of water tracks (described in section 2) on the
824 hydrograph is tested. The first simulation is based on
825 the channel network depicted in Figure 2, whereas in the
826 second simulation the water tracks are leveled to the
827 adjacent surface elevation. The simulation indicates that
828 the existence of water tracks accelerates runoff and leads to
829 higher amplitudes in the hydrograph than would be present
830 without them. Including water tracks improves the simula-
831 tion result when compared to the measured hydrograph
832 [Schramm, 2005]. Concerning the impact of soil parameters
833 on subsurface flow, model studies reveal that the MDT has
834 the highest influence, followed by the porosity and the
835 hydraulic conductivity [Schramm, 2005].

836 5.4. Sensitivity of the Hydrological System Toward 837 Changes in Climate Conditions

838 [63] As arctic temperatures and precipitation increase,
839 there remains uncertainty on how the additional input of
840 freshwater will be partitioned into streamflow and evapo-
841 transpiration. The interactions are further complicated by a
842 contribution of melted ground ice to base flow when
843 increasing temperatures deepen the active layer during
844 summer. An open question is whether a change in climate
845 will lead to a drying of the soil or to wetter conditions.

846 [64] Global and regional climate models predict different
847 changes for the future climate state of the arctic depending
848 on the warming scenario as well as on model performance.

Regardless of the unanswered question, which scenario is 849
the most likely one, changes on the hydrology can be 850
investigated by presuming various conditions and using 851
those as an input to model simulations. This was done in 852
this study for different climate change scenarios (see 853
Table 3) that include a change in three parameters: (1) the 854
summer temperature, (2) the summer precipitation, and (3) 855
the maximum depth of thaw. 856

[65] 2001 is used as the reference year, i.e., all changes of 857
the above-mentioned parameters are relative to the observed 858
climate conditions in 2001. Thus changes in the output, 859
such as simulated runoff and evapotranspiration, can be 860
compared to the 2001 simulation based on the real data set. 861
Simulations were executed only for the summer season, 862
lasting from 15 June until 13 September. The change in 863
precipitation was distributed equally over the summer 864
season, sustaining the range between minimum and maxi- 865
mum precipitation rates. For simplification the assumption 866
of a 10 cm (20 cm) deepening of MDT by a 2°C warming 867
was based on a study by Kane *et al.* [1991a]. The authors 868
determine that a gradual but steady warming of 2°C would 869
lead to a deepening of 10 cm (20 cm) after 20 a (45 a). 870

[66] Results indicate that a warming of 2°C without 871
additional precipitation results in a higher *R/P* and *ET/P* 872
ratio [Schramm, 2005]. Here the increase in runoff is 873

Table 3. Climate Change Scenarios A, C, and E and Their t3.1
Changes in Mean Summer Temperature, Precipitation, and
Maximum Depth of Thaw, Relative to the Observed Conditions
in 2001

Scenario	A 10	A 20	C 10	C 20	E 10	E 20	t3.2
Temperature, °C	+2	+2	+2	+2	+2	+2	t3.3
Precipitation, %	-	-	+8	+8	-10	-10	t3.4
Maximum depth of thaw, cm	58	68	58	68	58	68	t3.5
Change in storage compared to 2001, mm	-7.8	-10.7	-3.5	-6.2	-7.9	-10.8	t3.6

874 generated by a contribution of ground ice melted due to a
875 deeper thaw depth. Runoff is significantly higher in the
876 scenarios where an increase of precipitation is superimposed
877 over the warming. The opposite accounts for the scenarios
878 where precipitation input is decreased. All scenarios indi-
879 cate an increased loss in storage compared to the reference
880 amount in 2001, ranging from -3.5 to -10.8 mm. This
881 indicates that the enhanced evapotranspiration overwhelms
882 the increase in precipitation and results in a drying of the
883 soil.

885 6. Conclusions

886 [67] This study presented the application of the hydro-
887 logical model TopoFlow to Imnavait Creek, Alaska. Results
888 indicate that the model is an excellent tool for simulating the
889 overall water and energy balances of an arctic watershed.
890 The model performs quantitatively well, with measured and
891 simulated discharges being in a good agreement. The
892 different components of the water cycle, i.e., evapotranspi-
893 ration, snow melt, infiltration, and runoff, are well repre-
894 sented in the model, revealing that the model is able to
895 handle the seasonal change in meteorological conditions.
896 Some refinements are possible in the qualitative reproduc-
897 tion of some subprocesses: The onset of simulated snow-
898 melt discharge occurs distinctly earlier than the measured
899 discharge (7 d). This difference is in part due to the process
900 of snow damming, which is not understood well enough to
901 be incorporated into the model. Furthermore, the simulated
902 summer hydrograph shows deviations from the recordings:
903 Simulated discharge often leads site data; measured peak
904 discharges are usually lower and have a longer recession
905 time. This reveals that the model could be further refined in
906 the small-scale, short-term reproduction of storage-related
907 processes. Those can be attributed to the following facts: (1)
908 The channel grid used in the simulation does not consider
909 the ponds of the beaded stream system; (2) the spatial
910 variability of the active layer depth is not represented in
911 the simulation; and (3) the instantaneous infiltration used in
912 the modeling simplifies the complex soil moisture distribu-
913 tion on short-term scales. Finally, simulation results could
914 possibly be improved by spatially distributing several input
915 variables (now possible in the model), such as snow depth,
916 α_{PT} of the Priestley-Taylor method, the meteorological
917 variables, and the soil parameters during the thawing
918 season.

919 [68] Sensitivity studies reveal that the model is highly
920 sensitive to the initial height of the water table that is given
921 as an input to start the simulation. Even though this
922 sensitivity is realistic, it requires calibration which naturally
923 includes a source of error, as measurements are usually not
924 available in full detail.

925 [69] While various studies present projected climate
926 changes in the arctic, there remains uncertainty of how
927 these changes will impact the hydrological cycle, resulting
928 in enhanced or diminished runoff and soil moisture. This in
929 turn is likely to affect the biogeochemistry and/or ecology
930 of these systems (e.g., via changes in heat and water fluxes,
931 vegetation cover, etc.). It is possible and desirable to couple
932 TopoFlow with other models, and the authors encourage
933 this development. This study shows that TopoFlow is a

powerful tool for answering the question of how climate 934
change will affect the sensitive wetlands of arctic tundra. 935

Notation

C_0	degree day melt factor, mm/d °C.
ET/P	evapotranspiration to precipitation ratio, no units.
R/P	runoff to precipitation ratio, no units.
T_0	temperature of snow for isothermal conditions, °C.
α_{PT}	alpha parameter controlling the thaw depth, no units.
α_{TD}	alpha parameter for the Priestley-Taylor equation, no units.
z_0	surface roughness length, m.

[70] **Acknowledgments.** We gratefully acknowledge financial sup- 953
port by the U.S. National Science Foundation Arctic System Science 954
program (OPP-0229705). Special thanks are due to Robert Gieck, Pier 955
Paul Overduin, and Peter Prokein for their support in the preparation and 956
interpretation of field data. The two anonymous reviewers are thanked for 957
their constructive comments that helped improve this paper. 958

References

- 959
- ACIA (2004), *Impacts of a Warming Arctic: Arctic Climate Impact Assess-* 960
ment, 1042 pp., Cambridge Univ. Press, New York.
- Berezovskaya, S., D. L. Kane, and L. D. Hinzman (2005), Snowmelt hy- 961
drology of a headwater arctic basin revisited, *Eos Trans. AGU*, 85(47), 962
Fall Meet. Suppl., Abstract C41A-0195.
- Bergström, S. (1976), Development and application of a conceptual runoff 963
model for Scandinavian catchments, *SMHI Rep. RHO-7*, Swed. Meteorol. 964
and Hydrol. Institut., Norrköping, Sweden. 965
- Boike, J., K. Roth, and P. P. Overduin (1998), Thermal and hydrologic 966
dynamics of the active layer at a continuous permafrost site, *Water Res-* 967
sour. Res., 34(3), 355–363. 968
- Bolton, W. R. (2006), Dynamic modeling of the hydrologic processes in 969
areas of discontinuous permafrost, Ph.D. thesis, 163 pp., Univ. of Alaska 970
Fairbanks, Fairbanks, Alaska. 971
- Bolton, W. R., D. L. Hinzman, and K. Yoshikawa (2000), Stream flow 972
studies in a watershed underlain by discontinuous permafrost, in *Water* 973
Resources in Extreme Environments, edited by D. L. Kane, pp. 31–36, 974
Am. Water Resour. Assoc. Proc., Anchorage, Alaska. 975
- Bowling, L. C., D. L. Kane, R. E. Gieck, L. D. Hinzman, and D. P. 976
Lettenmaier (2003), The role of surface storage in a low-gradient arctic 977
watershed, *Water Resour. Res.*, 39(4), 1087, doi:10.1029/ 978
2002WR001466. 979
- Church, M. (1974), Hydrology and permafrost with reference to northern 980
North America, in *Permafrost Hydrology, Proceedings Workshop Semi-* 981
nar, pp. 7–20, Can. Natl. Comm., Int. Hydrol. Decade, Environ. Canada, 982
Ottawa, Ont., Canada. 983
- Dingman, L. S. (1973), Effects of permafrost on stream characteristics in 984
the discontinuous permafrost zone of central Alaska, in *Permafrost*, 985
North American Contribution to the Second International Conference, 986
Washington D. C., pp. 447–453, Natl. Acad. of Sci., Washington, D. C. 987
- Emmett, W. W. (1970), The hydraulics of overland flow on hillslopes, *U. S.* 988
Geol. Surv. Prof. Pap., 662-A, 68 pp. 989
- Hastings, S. J., S. A. Luchessa, W. C. Oechel, and J. D. Tenhunen (1989), 990
Standing biomass and production in water drainages of the foothills of the 991
Philip Smith Mountains, Alaska, *Holarct. Ecol.*, 12, 304–311. 992
- Hinzman, L. D., and D. L. Kane (1992), Potential response of an arctic 993
watershed during a period of global warming, *J. Geophys. Res.*, 97, 994
2811–2820. 995
- Hinzman, L. D., J. D. Fox, and D. L. Kane (1990), Soil freezing in a 996
subarctic deciduous forest, in *International Frozen Soil Symposium*, 997
21–22 March 1990, Spokane, Washington, edited by K. R. Cooley, 1000
CRREL Spec. Rep. 90-1, pp. 21–30, U.S. Army Cold. Reg. Res. and 1001
Eng. Lab., Hanover, N. H. 1002
- Hinzman, L. D., D. L. Kane, R. E. Gieck, and K. R. Everett (1991), 1003
Hydrologic and thermal properties of the active layer in the Alaskan 1004
arctic, *Cold Reg. Sci. Technol.*, 19, 95–110. 1005
- Hinzman, L. D., D. Wendler, R. E. Gieck, and D. L. Kane (1993), Snow- 1006
melt at a small Alaskan arctic watershed: 1. Energy related processes, in 1007
Proceedings of the 9th International Northern Research Basins Sym- 1008
posium/Workshop Canada 1992, edited by T. D. Prowse, C. S. Ommanney, 1009
and K. Ulmer, vol. 1, *NHRI Symp. 10*, pp. 171–226, Natl. Hydrol. Res. 1010
Inst., Saskatoon, Saskatchewan, Canada. 1011

- 1012 Hinzman, L. D., D. L. Kane, and Z. Zhang (1995), A spatially distributed
1013 hydrologic model for arctic regions, *International GEWEX Workshop on*
1014 *Cold-Season/Region Hydrometeorology, Summary Report and Proceed-*
1015 *ings, 22–26 May 1995, Banff, Alberta, Canada, Int. GEWEX Proj. Off.*
1016 *Publ. Ser. 15*, pp. 236–239, Washington, D. C.
- 1017 Hinzman, L. D., D. L. Kane, C. S. Benson, and K. R. Everett (1996),
1018 Energy balance and hydrological processes in an arctic watershed, in
1019 *Landscape Function and Disturbance in Arctic Tundra, Ecol. Stud.*,
1020 vol. 120, edited by J. F. Reynolds and J. D. Tenhunen, pp. 131–154,
1021 Springer, Berlin.
- 1022 Hinzman, L. D., et al. (2005), Evidence and Implications of recent climate
1023 change in northern Alaska and other arctic regions, *Clim. Change*, 72,
1024 251–298.
- 1025 Hinzman, L. D., R. W. Bolton, K. Petrone, J. Jones, and P. Adams (2006),
1026 Watershed hydrology and chemistry in the Alaskan boreal forest: The
1027 central role of permafrost, in *Alaska's Changing Boreal Forest*, edited by
1028 F. S. Chapin III et al., pp. 269–284, Oxford Univ. Press, New York.
- 1029 Kane, D. L., and L. D. Hinzman (1988), Permafrost hydrology of a small
1030 arctic watershed, in *Fifth International Conference on Permafrost*, edited
1031 by K. Senneset et al., pp. 590–595, Tapir Publ., Trondheim, Norway.
- 1032 Kane, D. L., L. D. Hinzman, C. S. Benson, and K. R. Everett (1989),
1033 Hydrology of Innavait Creek, an arctic watershed, *Holarct. Ecol.*, 12,
1034 262–269.
- 1035 Kane, D. L., R. E. Gieck, and L. D. Hinzman (1990), Evapotranspiration
1036 from a small Alaskan arctic watershed, *Nordic Hydrol.*, 21, 253–272.
- 1037 Kane, D. L., L. D. Hinzman, and J. Zarling (1991a), Thermal response of
1038 the active layer in a permafrost environment to climatic warming, *Cold*
1039 *Reg. Sci. Technol.*, 19(2), 111–122.
- 1040 Kane, D. L., L. D. Hinzman, C. S. Benson, and G. E. Liston (1991b), Snow
1041 hydrology of a headwater arctic basin: 1. Physical measurements and
1042 process studies, *Water Resour. Res.*, 27(6), 1099–1109.
- 1043 Kane, D. L., L. D. Hinzman, J. P. McNamara, Z. Zhang, and C. S. Benson
1044 (2000), An overview of a nested watershed study in arctic Alaska, *Nord.*
1045 *Hydrol.*, 31(4/5), 245–266.
- 1046 Kane, D. L., K. M. Hinkel, D. J. Goering, L. D. Hinzman, and S. I. Outcalt
1047 (2001), Non-conductive heat transfer associated with frozen soils, *Global*
1048 *Planet. Change*, 29(3–4), 275–292.
- 1049 Kane, D. L., R. E. Gieck, D. C. Kitover, L. D. Hinzman, J. P. McNamara,
1050 and D. Yang (2004), Hydrologic cycle on the North Slope of Alaska, in
1051 *Northern Research Basins Water Balance, IAHS Publ.*, 290, 224–236.
- 1052 Maidment, D. R. (Ed.) (1992), *Handbook of Hydrology*, 1400 pp.,
1053 McGraw-Hill, New York.
- 1054 McCarthy, J. J., O. Canziani, N. A. Leary, D. J. Dokken, and K. S. White
1055 (Eds.) (2001), *Climate Change 2001: Impacts, Adaptation, and Vulner-*
1056 *ability*, 1032 pp., Cambridge Univ. Press., New York.
- 1057 McNamara, J. P. (1997), A nested watershed study in the Kuparuk River
1058 basin, arctic Alaska: Streamflow, scaling, and drainage basin structure,
1059 Ph.D. diss., Univ. of Alaska, Fairbanks.
- 1060 McNamara, J. P., D. L. Kane, and L. D. Hinzman (1998), An analysis of
1061 streamflow hydrology in the Kuparuk River basin, arctic Alaska: A
1062 nested watershed approach, *J. Hydrol.*, 206, 39–57.
- 1063 Mendez, J., L. D. Hinzman, and D. L. Kane (1998), Evapotranspiration
1064 from a wetland complex on the arctic coastal plain of Alaska, *Nord.*
1065 *Hydrol.*, 29(4/5), 303–330.
- 1066 O'Callaghan, J., and D. Mark (1984), The extraction of drainage networks
1067 from digital elevation data, *Comput. Vision Graphics Image Process.*,
1068 28(3), 323–344.
- 1069 Osterkamp, T. E., and V. Romanovsky (1999), Evidence for warming and
1070 thawing of discontinuous permafrost in Alaska, *Permafrost Periglacial*
1071 *Processes*, 10, 17–37.
- Oswood, M. W., K. R. Everett, and D. M. Schell (1989), Some physical and
1072 chemical characteristics of an arctic beaded stream, *Holarct. Ecol.*, 12,
1073 290–295.
- Overduin, P. P. (2005), The physical dynamics of patterned ground in the
1075 northern foothills of the Brooks Range, Alaska, Ph.D. thesis, 182 pp.,
1076 Univ. of Alaska, Fairbanks, Fairbanks, Alaska.
- Priestley, C. H. B., and R. J. Taylor (1972), On the assessment of surface
1078 heat flux and evaporation using large-scale parameters, *Mon. Weather*
1079 *Rev.*, 100, 81–92.
- Quinton, W. L., D. M. Gray, and P. Marsh (2000), Subsurface drainage from
1081 hummock-covered hillslopes in the arctic-tundra, *J. Hydrol.*, 237(1–2),
1082 113–125.
- Reynolds, J., and J. D. Tenhunen (Eds.) (1996), *Landscape Function and*
1084 *Disturbance in Arctic Tundra, Ecol. Stud.*, vol. 120, edited by J. F.
1085 Reynolds and J. D. Tenhunen, 437 pp., Springer, Berlin.
- Romanovsky, V., M. Burgess, S. Smith, K. Yoshikawa, and J. J. Brown
1087 (2002), Permafrost temperature records: Indicators of climate change,
1088 *EOS Trans. AGU*, 83(50), 589–594.
- Rouse, W. R., P. F. Mills, and R. B. Stewart (1977), Evaporation in high
1090 latitudes, *Water Resour. Res.*, 13(6), 909–914.
- Schramm, I. (2005), Hydrologic modeling of an arctic watershed, Alaska,
1092 M. S. thesis, 108 pp., Univ. of Potsdam, Germany.
- Serreze, M. C., J. E. Walsh, F. S. Chapin III, T. Osterkamp, M. Dyurgerov,
1094 V. Romanovsky, W. C. Oechel, J. Morison, T. Zhang, and R. G. Barry
1095 (2000), Observational evidence of recent change in the northern high-
1096 latitude environment, *Clim. Change*, 46, 159–207.
- Slaughter, C. W., and D. L. Kane (1979), Hydrologic role of shallow
1098 organic soils in cold climates, paper presented at the Canadian Hydrology
1099 Symposium, Natl. Res. Council of Can., Ottawa, Canada.
- Smith, L. C., Y. Sheng, G. M. McDonald, and L. D. Hinzman (2005),
1101 Disappearing arctic lakes, *Science*, 308(5727), 1429.
- Stieglitz, M., J. Hobbie, A. Giblin, and G. Kling (1999), Hydrologic mod-
1103 eling of an arctic tundra watershed: Toward pan-arctic predictions,
1104 *J. Geophys. Res.*, 104, 507–518.
- Vörösmarty, C. J., L. D. Hinzman, B. J. Peterson, D. H. Bromwich, L. C.
1106 Hamilton, J. Morison, V. E. Romanovsky, M. Sturm, and R. S. Webb
1107 (2001), *The Hydrologic Cycle and Its Role in the Arctic and Global*
1108 *Environmental Change: A Rationale and Strategy for Synthesis Study*,
1109 84 pp., Arct. Res. Consortium of the U. S., Fairbanks, Alaska.
- Walker, D. A., E. Binnian, B. M. Evans, N. D. Lederer, E. Nordstrand, and
1111 G. W. Petersen (1989), Terrain, vegetation and landscape evolution of the
1112 R4D research site, Brooks Range Foothills, Alaska, *Holarct. Ecol.*, 12,
1113 261–283.
- Walsh, J. E., et al. (2005), Cryosphere and hydrology, in *Arctic Climate*
1115 *Impact Assessment*, chapter 6, pp. 181–242, Cambridge Univ. Press,
1116 London.
- Woo, M. (1986), Permafrost hydrology in North America, *Atmos. Ocean*,
1118 24(3), 210–234.
- Woo, M., and P. Steer (1983), Slope hydrology as influenced by thawing of
1120 the active layer, Resolute N.W.T., *Can. J. Earth Sci.*, 20(6), 978–986.
- Zhang, Z., D. L. Kane, and L. D. Hinzman (2000), Development and
1122 application of a spatially-distributed arctic hydrological and thermal pro-
1123 cess model (ARHYTHM), *Hydrol. Processes*, 14, 1017–1044.
- J. Boike and I. Schramm, Alfred Wegener Institute for Marine and Polar
1126 Research, Research Unit Potsdam, Telegrafenberg A43, 14473 Potsdam,
1127 Germany. (jboike@awi-potsdam.de)
- W. R. Bolton, Water and Environmental Research Center, P.O. Box
1129 755860, University of Alaska, Fairbanks, AK 99775-5860, USA.
- L. D. Hinzman, International Arctic Research Center, P.O. Box 757340,
1131 University of Alaska, Fairbanks, 99775-7340, USA.